Magnetic Particle Imaging for Biomedical Applications

Othman, Nurmiza Binti
Graduate School of Information Sclence and Electrical Engineering, Kyushu University

Tsubaki, Takuya
Graduate School of Information Sclence and Electrical Engineering, Kyushu University

Yoshida, Takashi
Faculty of Information Science and Electrical Engineering, Kyushu University

Enpuku, Keiji
Faculty of Information Science and Electrical Engineering, Kyushu University

https://doi.org/10.15017/20053

出版情報：九州大学大学院システム情報科学紀要. 16 (2), pp.51-56, 2011-09-26. 九州大学大学院システム情報科学研究院
バージョン：
権利関係：

九州大学大学院
システム情報科学紀要
第 16 巻　第 2 号　平成 23 年 9 月

Research Reports on Information Science and
Electrical Engineering of Kyushu University
Vol.16, No.2, September 2011

Magnetic Particle Imaging for Biomedical Applications

Nurmiza Binti OTHMAN*, Takuya TSUBAKI*, Takashi YOSHIDA**and Keiji ENPUKU**

(Received July 19, 2011)

Abstract: An imaging technique for the detection of magnetic nanoparticles (MNPs) has been studied for biomedical applications. First, a detection system, which measures the second harmonic signal from the MNPs, was designed and developed based on nonlinear properties of the MNPs under strong excitation field. By measuring the second harmonic signal, interference of the excitation field can be significantly reduced, when compared to the case of measuring the fundamental signal. Using this system, we could detect 100 μg of MNPs which were located at $z = 30$ mm under the detection coil. The detected signal field was 128 pT at the measurement frequency of 38.6 kHz, and the signal to noise ratio was as high as 10. Next, a field map from the MNPs was measured, and a clear contour map was obtained. The obtained contour map agreed well with numerical simulations. Using the contour map, we could directly estimate the position of markers. Finally, a field map from two markers, which were separated with a distance Δx, was measured in order to study the ability of position identification of two markers. It was shown that we could distinguish two markers located at $z = 20$ mm if they were separated by $\Delta x = 20$ mm. This simple detection system could be applied for the detection of sentinel lymph node during the biopsy.

Keywords: Magnetic nanoparticles, Bio-imaging system, Sentinel Lymph Node Biopsy, Magnetic sensor

1. Introduction

Magnetic markers, which are composed of polymer-coated magnetic nanoparticles (MNPs), have been studied for biological applications. Since MNPs can be easily controlled by external field excitation, this advantage has been used to extend novel techniques for various applications[1]. For instance, the applications in biological field are such as magnetic immunoassay, magnetic resonance imaging, drug delivery, magnetic hyperthermia, and magnetic particle imaging (MPI).

The MPI is a new imaging technique of MNPs detection for in-vivo applications. It is based on tomographic imaging technique to detect the signal field generated from the MNPs. Nonlinear properties of the MNPs under strong excitation field were used to achieve high spatial resolution. Numerous works have been extensively developed in order to improve the performance[2-7].

One of the applications of the MPI technique is the sentinel lymph node detection for breast cancer. Here, sentinel lymph node is defined as the first lymph node to which cancer cells are likely to be spread from the primary tumor before spreading to other lymph nodes. In order to detect the sentinel lymph node, MNPs were put into human body, and the signal from the MNPs was detected on the surface of the body. The positions of MNPs were identified by analyzing the contour map of the signal field.

In this study, we show the development of an MPI system for sentinel lymph node detection. First, we develop a detection system for MNPs which measures the second harmonic signal. By measuring the second harmonic signal, interference of the excitation field can be significantly reduced, when compared to the case of measuring the fundamental signal. Using this system, we could detect 100 μg of MNPs which were located at $z =$ 30 mm under the detection coil. Next, we measure the field map obtained from the MNPs in order to identify the marker position from the contour map. Finally, a field map from two markers, which were separated with a distance Δx, was measured in order to study the ability of position identification of two markers. It was shown that we could distinguish two markers located at $z = 20$ mm if they were separated by $\Delta x = 20$ mm.

2. MPI Technique for Sentinel Lymph Node Biopsy

Since our final goal is to develop an MPI system for the Sentinel Lymph Node Biopsy (SLNB), we briefly explain conventional methods for SLNB. SLNB is a procedure to determine the extent or stage of cancer, where the sentinel lymph node is removed and examined to determine whether cancer cells are present or not.

* Department of Electrical and Electronic Engineering, Graduate Student
** Department of Electrical Engineering

Present methods used for SLNB are such as radioactive substance and blue dye injection into the body (**Fig. 1**). However, allergy symptoms from blue dye injection and the risky from radiation exposure have been observed from these methods.

In order to solve this problem, magnetic marker, which is composed of polymer-coated magnetic nanoparticles (MNPs) as shown in **Fig. 2**, have been proposed as a new tracer instead of using both substances. The injected MNPs into the body are then been applied with external magnetic field, and resulted fields from the magnetized marker are detected by magnetic sensors at the body surface.

However, since the signal from a marker inside the body rapidly attenuates with the distance from the body surface, only extremely small field exists on the body surface; therefore, a system with a very sensitive magnetic sensor becomes as a needed in order to detect such a very small magnetic field signal. It is also necessary to develop a method to estimate the position of the MNPs from the contour map of the signal field.

3. Experimental

3.1 Magnetic Response of MNPs

It is well-known that MNPs show the super-paramagnetic behavior. In the absence of external magnetic field, the magnetic moment in each of MNPs randomly rotates owing to the thermal noise. Accordingly, the direction of the magnetic moment becomes random, and the mean value of the magnetic moment of the MNPs becomes zero. However, when MNP is magnetized under external field excitation, H, the magnetic moments in the MNPs tend to align in the direction of the H. As a result,

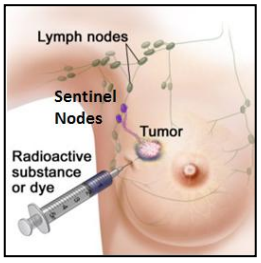

Fig. 1. Injection of substrates into the body for detection of sentinel lymph node[8].

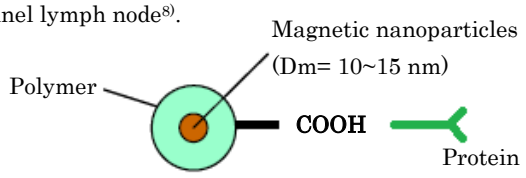

Fig. 2. Magnetic marker.

the mean magnetic moment of MNPs in the direction of H, which we define by $\langle m \rangle$, can be described by the following Langevin function[9],

$$\frac{\langle m \rangle}{m} = L\left(\frac{mH}{k_B T}\right) = \coth\frac{mH}{k_B T} - \frac{k_B T}{mH} \quad (1)$$

where L indicates the Langevin function, m is the magnetic moment of MNP, k_B is the Boltzmann constant and T is the absolute temperature.

In our experiment, we applied an external field which consists of the DC bias field H_{DC} and AC field $\sqrt{2}H_{AC}\cos(\omega t)$, thus resulting,

$$\frac{\langle m \rangle}{m} = \coth\left[\frac{H_{DC} - \sqrt{2}H_{AC}\cos(\omega t)}{k_B T/m}\right] - \frac{k_B T/m}{H_{DC} - \sqrt{2}H_{AC}\cos(\omega t)} \quad (2)$$

By expanding the right part of eq. (2) into Fourier series, we can obtain the n-th harmonic signal from super-paramagnetic MNPs, $\langle m \rangle_n$, as

$$\frac{\langle m \rangle_n}{m} = 2\omega\int_0^{1/\omega} L\left(\frac{H_{DC} - \sqrt{2}H_{AC}\cos(\omega t)}{k_B T/m}\right)\cos(n\omega t)dt \quad (3)$$

The properties of harmonic signals from MNPs are shown in **Fig. 3**. In **Fig. 3(a)**, amplitude of the harmonic signal from the MNPs is shown when DC and AC excitation field were applied. Here AC field was fixed at $\mu_0 H_{AC}$=1.0 mT and DC field $\mu_0 H_{DC}$ was varied in the range of 0 to 10 mT. The red, blue and green lines represent the output voltage of the inductive pickup coil for the fundamental, second, and third harmonic component, respectively.

As shown, the fundamental component decreased monotonically with H_{DC}. On the other hand, the second harmonic had a peak value at a certain value of H_{DC}. The peak value of the second harmonic component was about 1/4.4 times that of the fundamental one. Meanwhile, the third harmonic component showed a complicated dependence on H_{DC}. In addition, the value of H_{DC} at which signal peak had appeared, increased with an increase in H_{AC}[10].

Figure 3(b) shows the ratio of the peak value of the second harmonic component V_{2p} to that of the fundamental component V_{1p} for varying H_{AC}. As shown, V_{2p}/V_{1p} increased with increasing H_{AC} and gradually reached saturation. The value of V_{2p}/V_{1p} exceeded 10% when $\mu_0 H_{AC}$>0.5 mT, in which was about 20% for $\mu_0 H_{AC}$ = 1 mT.

Furthermore, we could see that the ratio V_{2p}/V_{1p} was roughly proportional to H_{AC} when H_{AC} was small. As the

fundamental component V_{1p} was proportional to H_{AC}, this relationship suggests the idea that the amplitude of the second harmonic V_{2p} became proportional to H_{AC}^2.

Here, we mention the merit of using the second harmonic signal instead of fundamental one. As shown later, an excitation field of about B_{ex}=1 mT is applied in the experiment. The signal field B_s from the sample is detected with a gradiometer coil, whose balance is about 100. This means that the gradiometer feels an interference field of B_{ex}/100=10 μT. On the other hand, the fundamental component of the signal field becomes around 5 nT as shown later, which is 2000 times as small as the interference field. In this case, therefore, it is very difficult to measure the signal field due to the large interference field. This problem can be avoided when we measure the second harmonic signal. In this case, we can separate the signal field from the interference one in the frequency domain.

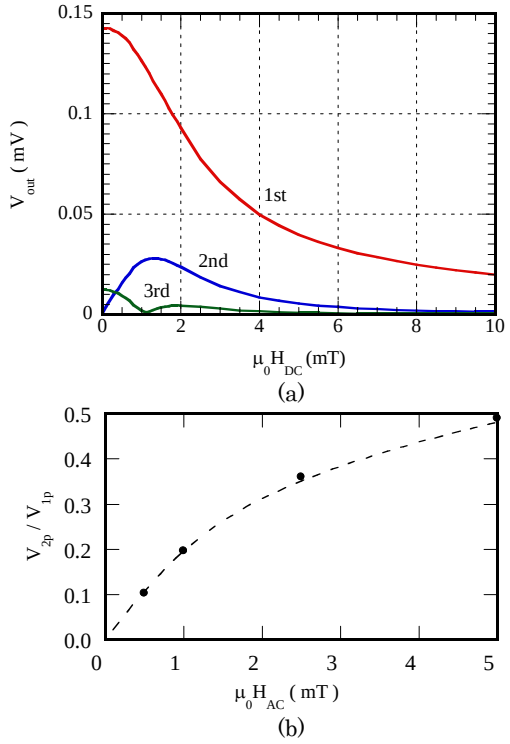

Fig. 3. (a) Harmonic signal from the MNPs when DC and AC excitation field were applied. Here AC field was fixed at $\mu_0 H_{AC}$=1.0 mT and DC field H_{DC} was varied. (b) Ratio of the peak value of the second harmonic component V_{2p} to that of the fundamental component V_{1p} for varying H_{AC}.

3.2 Experimental Setup

The focus of this study is to develop an MPI system which uses the second harmonic signal for the detection of the MNPs. **Figure 4** shows the schematically illustrated experimental setup, and **Fig. 5** shows the closed-up image of the experimental setup. The system is composed of an excitation coil, pickup coil gradiometer as the detection coil, magnetic marker, power amplifier and Lock-in amplifier.

Here, we used Resovist®, a commercial MNPs produced by the Bayer Schering Pharma, as the magnetic marker. Resovist is composed of carboxydextran-coated super-paramagnetic iron oxide (SPIO) particles, whose diameter is in the range of several nm to 30 nm. It is used as a contrast agent in magnetic resonance imaging. By coating with carboxydextran, the SPIO will be prevented from get aggregated and the compound can be highly hydrophilic[11]. Resovist used in this experiment was a colloidal solution with a concentration of 27.9 mg Fe/ml. The solution of 4 μl was diluted in 12 μl pure water to obtain sample with weight of 100 μg Fe. Then the marker was placed into a cell in **Fig. 5** with diameter Φ of approximately 5 mm.

An excitation field $H = H_{DC} + \sqrt{2}H_{AC}\cos(2\pi ft)$ was applied via an excitation coil to the magnetic marker. We constructed an excitation coil with an inner diameter of 20 mm and an outer diameter of 70 mm. The number of turns of the excitation coil was 346.

The signal from the magnetized marker was detected at the detection coil which was installed concentrically with the excitation coil. Here, the average diameter and the number of turns of the pickup coil were d_p = 8 mm and n_p = 85, respectively. The pickup coil was formed to act as the first-order gradiometer in order to avoid the interference of the excitation field, and the baseline of the gradiometer was set as 33 mm.

In the experiment, we fixed both the DC and AC excitation current at 1A in order to obey the relationship $H_{DC} = H_{AC}$[10]. It was shown previously that the peak value of the second harmonic signal can be obtained under such condition. The frequency of the AC excitation field was chosen as f= 19.3 kHz, giving the second harmonic signal frequency of 38.6 kHz. The second harmonic signal was extracted using the function provided in a lock-in amplifier. By using the second harmonic signal detection, we have successfully avoided interference from the excitation field.

The magnetic marker was placed on a plate which was moved by a xyz - stage. The distance z between magnetic marker and the detection coil was changed between the range of 10 to 30 mm, and accordingly both DC and AC

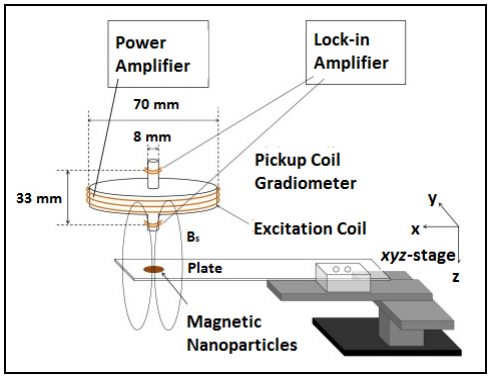

Fig. 4. Experimental setup.

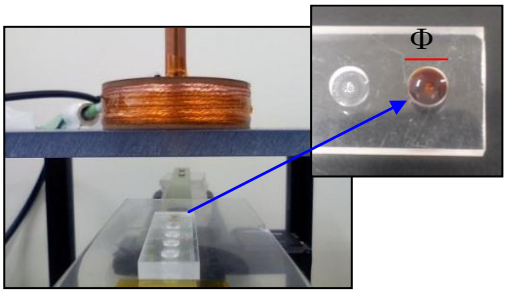

Fig. 5. Closed-up image of the experimental setup. The enlarged figure shows an image of liquid phase magnetic marker placed into a cell with diameter of 5 mm.

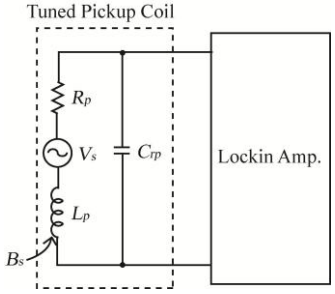

Fig. 6. Resonant circuit for the readout of pickup coil.

excitation fields onto the sample were changed from 2.4 to 0.8 mT.

In the present detection system, signal from the pickup coil was readout by using an LC resonant circuit as shown in **Fig. 6**. The second harmonic signal to be detected can be enhanced by a quality factor of Q. The resonant frequency f_{rp} of the pickup coil can be calculated as $f_{rp} = 1/\left(2\pi\sqrt{L_p C_{rp}}\right)$. Then we determined C_{rp} to obtain f_{rp} = 38.6 kHz. By using the parameters L_{p} = 0.11 mH, R_{p} = 3.6 Ω and f_{rp} = 38.6 kHz, we obtained $Q = 2\pi f_{rp} L_p / R_p = 7.4$. Hence, the sensitivity of the pickup coil became $2\pi f n_p \left(\pi d_p^2/4\right) Q =$ 7668 V/T at the resonant frequency of 38.6 kHz.

4. Results and Discussion

4.1 Detection of MNPs by Using the Second Harmonic Signal

First, we explored the sensitivity of the measurement system. **Figure 7** shows the relationship between the second harmonic signal detected at the pickup coil and the distance z between the pickup coil and the sample. Both DC and AC excitation currents were fixed at 1 A and z was changed from 10 to 30 mm. Open circles in **Fig. 7** represent the signal voltage V_{s2} across the pickup coil. Closed circles represent the signal field B_{s2} at the pickup coil, which is calculated with the sensitivity of 7668 V/T of the circuit.

As shown, we have successfully detected 100 μg MNPs which was located at z = 30 mm. This implies the ability of the system developed to detect the sentinel lymph node which is located at 30 mm under the body surface. In addition, B_{s2} was inversely proportional to z^6 with increasing z. Further explanation of this relationship was discussed in detailed in reference 10.

In **Fig. 7**, the minimum detectable signal voltage was V_{s2} = 979 nV when z = 30 mm. We took into account the sensitivity at the detection system as 7668 V/T and we obtained the minimum detectable B_{s2} was 128 pT. The lock-in amplifier used in the system consisted with the peak-to-peak value of the noise voltage of 60 nV when the time constant was set to be T_c = 10 ms. As the sensitivity of the detection coil was 7668 V/T at 38.6 kHz, we obtained the magnetic field noise as 7.8 pT. Therefore we could get the signal-to-noise ratio as high as 10 when the minimum detectable B_{s2} was 128 pT.

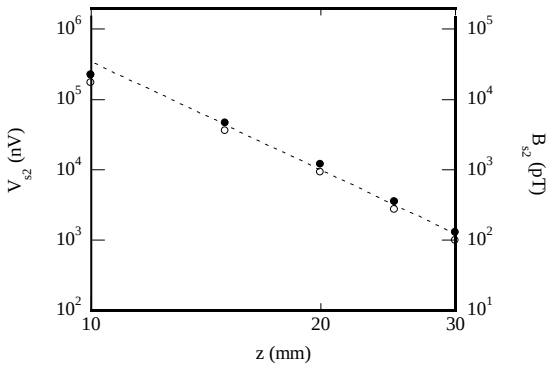

Fig. 7. Relationship between the second harmonic signal B_{s2} and the distance z, when both DC and AC excitation current were fixed at 1 A.

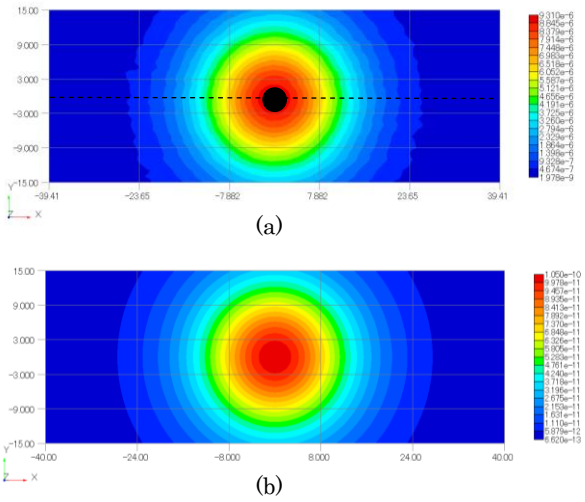

(a) (b)

Fig. 8. Contour map of the second harmonic signal detected from the sample located at $z = 20$ mm under the detection coil. (a) Experimental result, and (b) numerical simulation. Black circle in (a) represents the position and size of the sample.

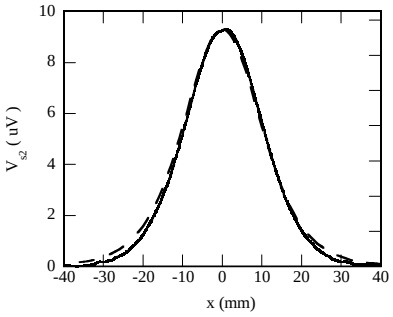

Fig. 9. Waveform of the detected signal when the sample was moved along the x-axis at $y = 0$, which corresponds to the broken line in **Fig. 8(a)**. Solid and dashed lines represent the experimental result and numerical simulation respectively.

4.2 Field Map Measurement

Next, we measured the field map from the magnetized MNPs, in which detected signals were plotted as a contour map for imaging. This contour map can be used to estimate the position of the sample in the xy plane. We defined $x = y = 0$ as the origin of the sample position, in which sample was placed just under the pickup coil.

Figure 8(a) shows the measured contour map of signal field B_{s2} from the MNPs for $z = 20$ mm. The excitation field $\mu_0 H_{DC}$ and $\mu_0 H_{AC}$ at the sample was calculated to be 1.3 mT. The sample was moved in the x -direction at a speed of 20 mm/s and the B_{s2} was detected at intervals of 1 mm from $y = -15$ mm to 15 mm. As a result, we could obtain a clear contour map as shown in **Fig. 8(a)**. It had a peak value at $x = y = 0$, indicating the possibility of direct estimation for real position of the sample from the contour map.

Figure 9 shows the waveform of the detected signal V_{s2} when the sample was moved in the x -direction at $y = 0$ in which corresponds to the broken line shown in **Fig. 8(a)**. The solid line in **Fig. 9** represents the experimental result. As shown in this figure, detected signal had a peak value of 9.24 μV at $x = 0$, giving the evidence that the sample was placed just under the pickup coil.

We also compared the experimental results with the numerical simulation in order to study the precision of the field map. **Figure 8(b)** shows the simulation result of the contour map of the signal field. As shown, the experimentally obtained contour map shown in **Fig. 8(a)** agreed well with the numerical simulation.

The dashed line in **Fig. 9** shows the simulation result of the waveform when the sample was moved in the x -direction at $y = 0$. The experimental result indicated by the solid line in **Fig. 9** agreed well with the simulation. These agreements indicate that the field maps from the MNPs were obtained with high precision in the present experiment.

4.3 Detection of MNPs from Two Samples

In order to study the ability of position identification of two markers, we also performed an experiment for detection of two samples by using the same system. **Figure 10** shows an example of image of two samples which were separated by $\Delta x = 10$ mm. For measurement, we used two samples with similar size and type as were used in previous experiment.

The distance Δx between two samples was varied from 10 mm to 25 mm. The depth of the samples was set as z =20 mm under the pickup coil. As a result, we could successfully identify two samples when they were separated by Δx = 20 mm. **Figure 11(a)** shows the measured field map from the two samples. We could see clear double peaks of the signal field. The peak position of the signal field agreed with the position of the samples. Therefore, we could successfully distinguish two samples.

We also compared the field map with the numerical simulation. **Figure 11(b)** shows the simulation result of the contour map. As shown, the measured contour map agreed well with numerical simulations. The existence of double peaks at two different positions was successfully observed in both maps.

Figure 12 shows the waveform of detected signal when both samples were moved in the x -direction at $y = 0$ in which corresponds to the broken line shown in **Fig. 11(a)**. The solid line represents the experimental result, while the dashed line is the calculated ones. We could see that double peaks appeared approximately at $x = 0$ mm and $x = 20$ mm, individually. This might indicates the real position of MNPs in both samples which accumulate in the two sentinel lymph nodes under the body surface.

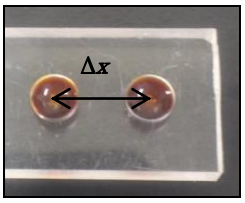

Fig. 10. Image of two samples with diameter Φ of approximately 5 mm and were separated by $\Delta x = 10$ mm.

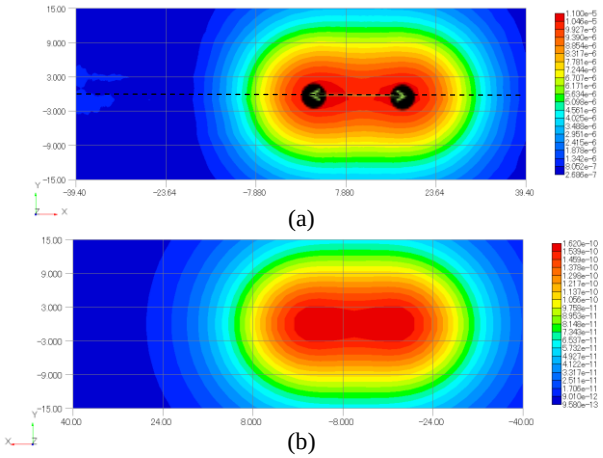

Fig. 11. Contour map of the second harmonic signal detected from two samples separated by $\Delta x = 20$ mm and located at $z = 20$ mm under the detection coil. (a) Experimental result, and (b) numerical simulation. Black circles in (a) represent the position and size of the samples.

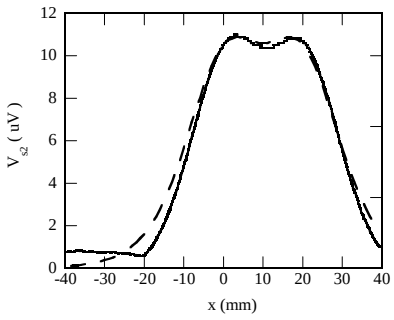

Fig. 12. Waveform of the detected signal when samples were moved along the x axis at $y = 0$. Solid and dashed lines represent the experimental result and numerical simulation, respectively.

5. Conclusion

We developed a system for MNPs imaging by using the second harmonic signal detection. First, we showed that a sample consists of 100 μg of MNPs was successfully detected with the experimental setup using the resonance type pickup coil with detection sensitivity of 7668 V/T at signal frequency of 38.6 kHz. The second harmonic signal detected was about 128 pT when sample was located at $z = 30$ mm under the detection coil. Then we showed that the position of the sample could be directly estimated from the contour map obtained. Finally, we showed that we could distinguish two samples located at $z = 20$ mm under the detection coil if they were separated by $\Delta x = 20$ mm. The experimental results agreed well with the numerical simulation. This simple detection system may give contribution to the in-vivo applications, especially to the identification of sentinel lymph node during the biopsy.

References

1) Q. A. Pankhurst, et al., *J. Phys. D: Appl. Phys.*, **42**, 224001, 2009.
2) S. Tanaka, et al., *IEEE Trans. Appl. Supercond.*, **13**, No. 2, 377-380, 2003.
3) K. Enpuku, et al., *Physica C*, **469**, 1634-1637 2009.
4) M. P. Nikitin, et al., *J. Magn. Magn. Mat.*, **321**, no. 10, 1634-1637 2009.
5) B. Gleich, et al., *Nature*, **435**, 1214-1217, 2005.
6) J. B. Weaver, et al., *Med. Phys.*, **35**, 1988-1994, 2008.
7) T. F. Sattel, et al., *J. Phys. D: Appl. Phys.*, **42**, 022001, 2009.
8) National Cancer Institute (2010) Breast Cancer Treatment. Retrieved from http://www.cancer.gov/cancertopics/pdq/treatment/breast/Patient/page5#Keypoint21
9) S. Chikazumi et al., *Physics of Magnetism*, New York: Wiley, 1964.
10) T. Yoshida, et al., *IEEE Trans. Mag.* (To be published).
11) Schering AG (2002) Retrieved from http://radiologie-uni-frankfurt.de/sites/radiologie-uni-frankfurt.de/content/e43/e2321/e2331/resofinal_eng.pdf.